Supplementary Materials for

Detection of Magnetic Gap in Topological Surface States of $MnBi_2Te_4$

Hao-Ran Ji(季浩然)[1†], Yan-Zhao Liu(刘彦昭)[1†], He Wang(王贺)[2], Jia-Wei Luo(骆佳伟)[1], Jia-Heng Li(李佳恒)[3,4], Hao Li(李昊)[5,6], Yang Wu(吴扬)[6,7], Yong Xu(徐勇)[3,4,8], and Jian Wang(王健)[1,3,9,10,**]

[1]International Center for Quantum Materials, School of Physics, Peking University, Beijing 100871, China

[2]Department of Physics, Capital Normal University, Beijing 100048, China

[3]State Key Laboratory of Low-Dimensional Quantum Physics, Department of Physics, Tsinghua University, Beijing 100084, China

[4]Frontier Science Center for Quantum Information, Beijing 100084, China

[5]School of Materials Science and Engineering, Tsinghua University, Beijing 100084, China

[6]Tsinghua-Foxconn Nanotechnology Research Center and Department of Physics, Tsinghua University, Beijing 100084, China

[7]Department of Mechanical Engineering, Tsinghua University, Beijing 100084, China

[8]RIKEN Center for Emergent Matter Science (CEMS), Wako, Saitama 351-0198, Japan

[9]CAS Center for Excellence in Topological Quantum Computation, University of Chinese Academy of Sciences, Beijing 100190, China

[10]Beijing Academy of Quantum Information Sciences, Beijing 100193, China

I. Repeatable observations of the surface gap on multiple point contact states through PCTS measurements

The point contact spectra (PCS) showing the surface gap structure, as well as the linear conductance structure (LCS), are obtained from multiple point contact (PC) states. Fig. S1 shows six sets of PCS in different PC states using a platinum-iridium (PtIr) tip (a-b) or a niobium (Nb)

† These authors contributed equally to this work.
** Corresponding author: jianwangphysics@pku.edu.cn

tip (c-f). Fig. S1(a) is adapted from Fig. 2 (c) and (d) in the main text for comparison. The gap size, the transition temperature, and the corresponding contact resistance of each set of PCS are summarized in Table I. The surface gaps with consistent energy sizes (from 30 to 50 meV) and the transition temperatures (from 20 to 24 K) accord with the theoretical predicted magnetic gap on the surface of $MnBi_2Te_4$,[1] and demonstrate the reproducibility of the experimental observation of the surface gap of $MnBi_2Te_4$.

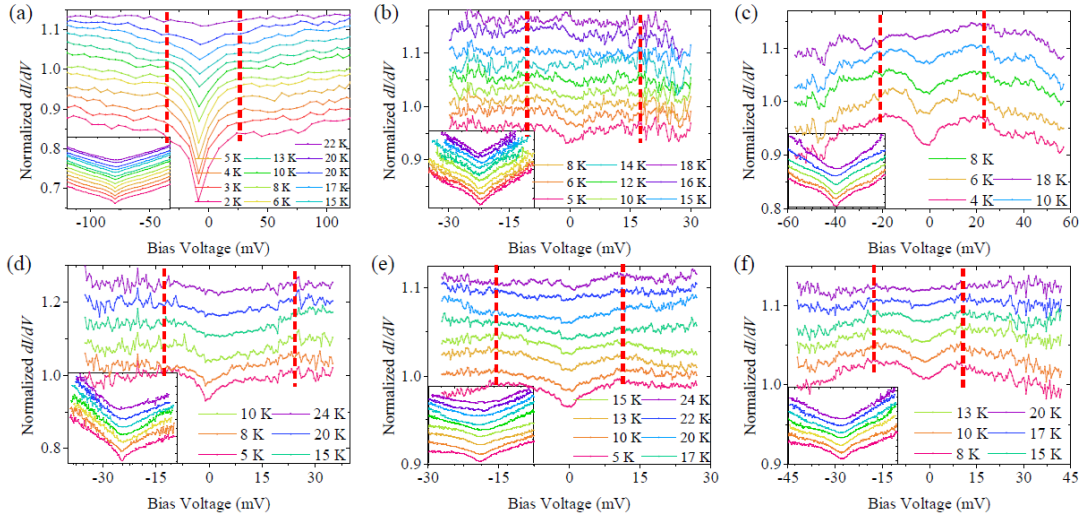

Fig. S1. The PCTS measurements on $MnBi_2Te_4$ single crystal. Normalized differential conductance (*dI/dV*) spectra after background-subtraction at selected temperatures obtained by a PtIr tip (a-b), or obtained by an Nb tip (c-f). The inset in each set of PCS represents the raw data. The spectra are shifted for clarity. The vertical dashed lines indicate the detected surface gap.

TABLE I. Statistical results of the detected gap structure including the gap size, the transition temperature, and the corresponding contact resistance.

Point contact state	Gap size	Transition temperature	Contact resistance
a	~50 meV (2 K)	~24 K	~699 Ω (2 K)
b	~30 meV (5 K)	~20 K	~445Ω (5 K)
c	~40 meV (4 K)	~20 K	~1254 Ω (4 K)
d	~35 meV (5 K)	~24 K	~1305 Ω (5 K)
e	~30 meV (5 K)	~24 K	~438 Ω (5 K)
f	~30 meV (8 K)	~20 K	~279 Ω (8 K)

II. Theoretical analysis for point contact Andreev reflection spectroscopy (PCARS) data shown in Fig. 4 of the main text

Fig. S2(a) represents the original PCS of Fig. 4 in the main text that has not been symmetrized. The double-peak structure is evident at low temperatures and the differential conductance (*dI/dV*) curves become flat above the superconducting transition temperature of Nb (T_c = 9.26 K). As shown in Fig. S2(b), the modified Blonder-Tinkham-Klapwijk (BTK) model without spin-polarization is applied for fitting. The corresponding parameters are shown in Fig. S2(c). The BCS fitting is also applied to the temperature-dependent value of Δ, shown in Fig. S2(c). The BCS fitting results give Δ = 1.38 meV (T = 0 K) and T_c = 9.9 K, obviously contradicting with the properties of Nb (Δ=1.53 meV, T_c=9.26 K). The inset of Fig. S2(c) shows the temperature-dependent values of the broadening parameter Γ (red) and the interface barrier strength Z (black). The maximum and minimum values of the parameter Z are 0.88 meV and 0.54 meV respectively. The large variation range of Z value is unreasonable since the parameter Z is supposed to be temperature-independent in the BTK fitting process. Most importantly, the ratio of Γ/Δ is around 80%, which is too large to be acceptable for BTK fitting results. Because the parameter Γ is related to the quasiparticle scattering rate and this parameter value should be smaller than superconducting gap Δ for the stabilization of the superconducting phase. Thus, the possibility that the typical PCS shown in Fig. S2(b) are mainly contributed by the large Z without P is excluded.

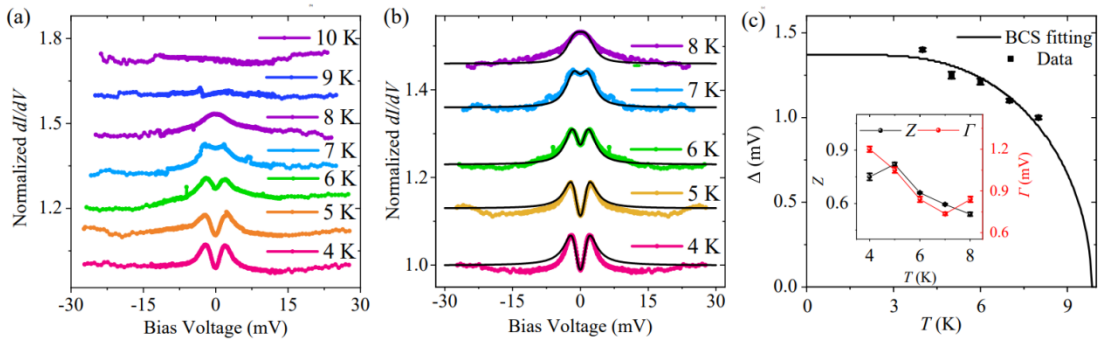

Fig. S2. The PCARS results and the conventional BTK fitting results of the PC state shown in Fig. 4 in the main text. (a) Normalized spectra at selected temperatures without symmetrizing process. (b) The symmetrized dI/dV spectra of (a). The solid lines are the best BTK fitting results without considering spin-polarization. The curves are shifted for clarity. (c) The squares are the Δ values

obtained from the conventional BTK fitting without spin-polarization. The solid line is the BCS fitting curve, giving a BCS ratio of $2\Delta/k_BT_c$=3.24. Inset in (c) shows the parameter Z and parameter Γ at different temperatures.

III. Spin polarized BTK fitting curves without shift

Selected PCARS data and corresponding spin-polarized fitting curves from Fig. 4(a) are shown in Fig. S3 without shifts. The double-peak structure is well fitted, suggesting the good quality of fitting with the spin-polarized BTK model.

Theoretical BTK models are based on an ideal, ballistic, and one-dimensional point contact,[1] which may sometimes fail to describe the real condition comprehensively. For example, the critical current dips outside the superconducting double peaks, as one typical phenomenon in point contact measurements, cannot be fitted by present theoretical models.[3] Therefore, the traditional treatment of the fitting process is mainly focused on the double-peak feature and ignores the dips.[3,4] Considering this fitting criterion, the spin-polarized BTK model can well explain the experimental curves, since the double-peak structure can be well fitted.

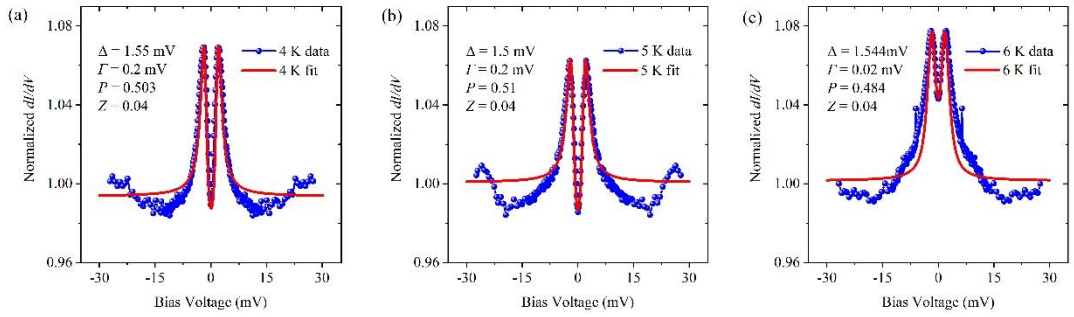

Fig. S3. Selected normalized spectra at (a) 4 K, (b) 5 K, and (c) 6 K from the data shown in Fig. 4. The solid lines are the spin-polarized BTK fitting curves of Fig. 4(a). The best-fit parameters are also shown in the figures.

IV. Comparison in the Γ and Δ behaviors between the spin polarized BTK fitting and the conventional BTK fitting

The Γ parameter is the broadening term in the conventional BTK model and spin-polarized BTK model, related to the shortening of the quasiparticle lifetime. Once the Γ is too large, the

lifetime of quasiparticles is too short for a stable superconducting phase and the superconductivity is expected to be substantially suppressed in the PC region in principle. Therefore, the Γ value is required to be much smaller than the energy gap Δ.

In our spin-polarized BTK fitting result, the Γ value is 0.2 meV from 4 K to 5 K, and the value is 0.02 meV from 6 K to 8 K. The largest ratio of Γ divided by Δ is about 13.3% and the smallest ratio is only 1.4% (shown in Fig. S4(a)). The Γ value is much smaller than the Δ value. Such fitting values are reasonable results for a ballistic PC measurement, which indicates that the electrons can transport through the contact with nearly no scattering. Small Γ values that are close to zero, or are exactly zero, have been reported in both conventional BTK fitting and spin polarized BTK fitting of ballistic PC measurements.[2-8]

By contrast, the largest ratio of Γ divided by Δ is about 85.7% and the smallest ratio is still 66.9% in the fitting result of the conventional BTK model without spin polarization (shown in Fig. S4(b)). The Γ parameter and the Δ value at each temperature have nearly the same magnitude of order.

The superconductivity conductance enhancement (compared to the conductance of normal state) in Fig. 4 is less than 10%, which is a general spectroscopic feature of PCARS with spin polarization.[2,6] The imbalance between spin-up and spin-down electrons suppresses the process of Andreev reflection and, consequently, suppress the superconducting enhancement in the PCS. In PC measurements without spin polarization, the conductance enhancements with a reasonably small Γ parameter are generally over 20% and sometimes are over 60%.[7,8] Therefore, conventional BTK fitting without spin polarization cannot explain our PCARS results.

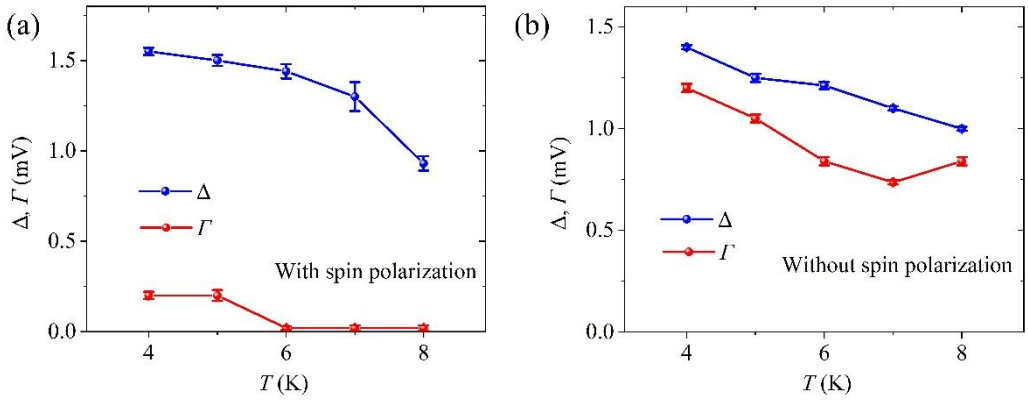

Fig. S4. Temperature dependence of the superconducting energy gap (Δ), and the broadening parameter (Γ) obtained through (a) the spin-polarized BTK fitting results of Fig. 4, and (b)

conventional BTK model fitting results of Fig. S2.

V. Comparison between our work and previous ARPES reports and theoretical works on the magnetic gap in the topological surface state of $MnBi_2Te_4$

Before our work, mainly ARPES measurements were carried out to detect the surface gap of the intrinsic topological insulator $MnBi_2Te_4$. The mostly probed surface is the (111) surface of $MnBi_2Te_4$, which is predicted to host gapped topological surface states.[1] A detailed comparison to the published results is shown in Table II. So far, only our work is consistent with the theoretical predictions in both the emergency temperature and the gap size.

TABLE II. Comparison between our work and published works on the gap structure of the topological surface states.

	Surface gap	Method	Note
Our work	~50 meV (2 *K*)	PCTS measurement	The gap closes around 24 *K*
Nature **576**, 416 (2019)	~70 meV (17 *K*)	ARPES measurement	The gap is still present at 35 *K*
Nature **576**, 416 (2019)	88 meV	Theoretical calculation	
Phys. Rev. Research **1**, 012011 (2019)	~85 meV (5 *K*)	ARPES measurement	The gap is still around 85 meV at 300 *K*
Sci. Adv. **5**: eaaw5685 (2019)	~50 meV	Theoretical calculation	
Phys. Rev. Lett. **122**, 206401 (2019)	~50 meV	Theoretical calculation	
Phys. Rev. X **9**, 041038 (2019)	Gapless	ARPES measurement	
Phys. Rev. X **9**, 041039 (2019)	Gapless	ARPES measurement	
Phys. Rev. X **9**, 041040 (2019)	Gapless	ARPES measurement	
Phys. Rev. Lett. **125**, 117205 (2020)	Gapless	ARPES measurement	

Note added: After our submission, we noticed a STM work on the bulk $MnBi_{2-x}Sb_xTe_4$, which reported a surface gap of 50 meV remaining unchanged in both antiferromagnetic (AFM) and ferromagnetic (FM) states.[9]

VI. Discussions about the tunneling regime point contact measurements

The point contact tunneling spectroscopy (PCTS) refers to the spectroscopy measured in PC junction with a relatively large contact barrier between sample and tip.[10,11] In the PCTS measurements, the electron tunneling is dominant in the electrical transport across the contact. Hence, through measuring the d*I*/d*V* spectra, PCTS can provide the electronic structure features of the detected samples.[12] Electronic gaps, like superconducting energy gap, charge density wave gap, and Kondo gap, can be studied by PCTS.[13-16]

First, in our measurements, an insulating oxide barrier is intentionally formed in the tip-sample interface by exposure to the atmosphere. It is a common treatment to take the native oxidized surfaces as the insulating barrier in tunneling measurements.[14,17] Correspondingly, our point contact resistances are very large, as shown in Table I. These results are consistent with the scenario of the tunneling point contact, whose resistances are usually from hundreds of ohms to thousands of ohms,[10,18] and are subsequently larger than typical metallic point contact whose resistances are about several ohms to tens of ohms.[19] In Table III, we summarize typical contact resistances obtained by tunneling measurements in previous reports which basically accord with our contact resistance values.

TABLE III. Typical contact resistances of the PCTS measurements in previous reports.

Reference	Techniques	Resistance values	Temperature
Phys. Lett. **20**, 581(1966)	PCTS with needle-anvil configuration	"*tunneling characteristics have been observed in junctions having resistances of less than 100 Ω to greater than 100 000 Ω*"	Not mentioned
J. Appl. Phys. 44, 3734 (1973)		Around 500 Ω	4.2 K

Physica B **218**, 185 (1996)		About 90 Ω	4.2 K
Acta Phys. Pol., A **93**, 355 (1997)		About 30 Ω	300 K
Phys. Rev. B **60**, 4624 (1999)		About 2000 Ω	77 K
Phys. Rev. Lett. **113**, 177004 (2014)		About 500 Ω	2.3 K
AIP Advances **8**, 125217 (2018)	PCTS with a filament contact realized by the nanofabrication	About 600 Ω	4.2 K
Nanoscale, **7**, 8531(2015)		In the range of 20~30 kΩ	Not mentioned

Second, LCS in a wide bias voltage range is observed in nearly all PCTS spectra. Normally, the LCS is ascribed to the inelastic tunneling process and is a signature of tunneling spectra.[20-23] For comparison, such LCS is absent in metallic PC.[19] In the inelastic tunneling process of PCTS, electrons tunnel through the barrier and scatter with the broad and flat distribution of energy-loss modes in the barrier, leading to the asymmetric LCS in the dI/dV spectra. The corresponding LCS follows$(\mathrm{d}I/\mathrm{d}V) \propto \int_0^{eV} F(E)dE$, where e$V$ is the electron energy and $F(E) \approx$ constant is the spectral distribution of inelastic modes in the barrier.[21,24] The LCS in the spectra indicates that the data are obtained in the tunneling regime.

Additionally, the thermal smearing behavior of our LCS is consistent with the inelastic tunneling scenario, which further confirms the tunneling is the main conduction mechanism in our PCTS measurements. As seen from the two dI/dV curves in Fig. 2(a) in the main text, at 6 K, there is a sharp minimum structure around zero bias voltage, which is smoothed out as the temperature increases to 24 K. This result is consistent with previous reports on tunneling measurements, where the sharp minimum structure of the LCS gradually smears out with increasing temperature.[21] The second derivative of conductance $\mathrm{d}^2G/\mathrm{d}V^2$ around zero bias is generally used to characterize this smearing. As shown in Fig. 2(b) in the main text, the $\mathrm{d}^2G/\mathrm{d}V^2$ around zero bias of our PCTS spectra exhibits a monotonic and linear temperature-dependence with a slope of approximately 6.1 k_BT (k_B is the Boltzmann constant). The linear fitting follows previous theoretical calculation of the thermal smearing analysis in tunneling measurements, where the

theoretical line goes through the origin.[21] This temperature-dependent behavior is in agreement with the theoretical calculation and experimental work on tunneling measurements with a slope of approximately 6 k_BT.[21] Actually, even no constraint is applied in the fitting process, the slope is still much larger than k_BT, and the inelastic tunneling appears to provide a natural explanation for this large thermal smearing. Thus, the LCS in the measured PCS indicates that our PCTS measurements are in the tunneling regime.

VII. Discussions about the origin of the gap structure in the PCTS measurements

Two decisive features of the gap structure in the PCTS measurements are that the gap emerges just below T_N (~ 24 K) and exhibits a gap size of 50 meV, in agreement with the theoretical prediction.[1]

According to the theoretical calculation, the ferromagnetism forms in each septuple layer of $MnBi_2Te_4$ and exhibits AFM coupling along the c-axis below T_N. The resultant out-of-plane ferromagnetism in the surface layer of $MnBi_2Te_4$ induces a gap in the topological surface states.[1] The gap structure in our spectra, emerging just below the antiferromagnetic-paramagnetic transition and diminishing as temperature increasing to T_N, accords with such theoretical prediction. Additionally, the transport spin-polarization and the magnetoresistance hysteresis obtained through PC measurements indicate the out-of-plane ferromagnetism in the surface and support the magnetism-induced gap in $MnBi_2Te_4$. The magnetoresistance hysteresis is observed through the point contact on the surface of $MnBi_2Te_4$ as shown in Fig. 3. By sweeping the out-of-plane magnetic field, the hysteretic behavior is also observed in $MnBi_2Te_4$ thin films with coercive fields slightly smaller than 1 T,[25,26] which is attributed to the surface ferromagnetism,[26] agreeing with our point contact scenario.

Excitations, like phonon, may also lead to spectra with some kink structures. Phonon mechanism, for example, does not agree with our spectra for the following reasons. Firstly, multiple kinks are generally observed in the point contact measurement as there are always multiple phonon modes,[4,27] which is at odds with our observations. Secondly, in point contact measurement, the phonon-induced features are generally studied through the second derivative of conductance d^2I/dV^2 spectra because the intensity of electron-phonon interaction is too small to be

distinguished in d*I*/d*V* spectra,[4,27] which contradicts with the clear and distinguishable structure in our d*I*/d*V* spectra. Additionally, the characteristic energy scale of the gap structure about 50 meV and the emergency just below T_N are consistent with the theoretical predictions about the surface gap.[1,28]

Point contact spectroscopy, as a surface sensitive measurement, mainly obtains the properties of the contact region on the sample surface.[30-32] As a magnetic topological insulator, $MnBi_2Te_4$ has a bulk bandgap around 200 meV, which does not change across the AFM transition.[1,29,30] Although contributions from bulk states cannot be fully excluded in PC measurement in principle, the 50 meV gap structure observed in PCTS measurements below T_N does not agree with the bulk bandgap. The consistencies with the predicted surface gap in energy size and magnetic origin can exclude other possibilities, including excitations that may not disappear around T_N, and the bulk gap which is as large as 200 meV,[1,29,30] etc. The combined results mentioned above indicate that a magnetic gap in the topological surface states is detected in our PCTS measurements.

VIII. Brief introduction about the spin polarized BTK model

Point contact measurement is a well-established probe for quantitatively measuring spin polarization in FM materials. In the superconducting point contact with a FM sample, the imbalance in the number of spin-up and spin-down electrons at the Fermi level of the sample will limit the Andreev reflection. The transport spin polarization quantity *P* can be defined as

$$P=\frac{N_{\uparrow}(E_F)v_{F\uparrow}-N_{\downarrow}(E_F)v_{F\downarrow}}{N_{\uparrow}(E_F)v_{F\uparrow}+N_{\downarrow}(E_F)v_{F\downarrow}},$$

where $N_{\uparrow}E_F$ and $N_{\downarrow}E_F$ are the spin-dependent density of states and $v_{F\uparrow}$ and $v_{F\downarrow}$ are corresponding Fermi velocity. Then, the total current can be divided into two parts: $I=(1-P)I_u+PI_P$. I_P (I_u) denotes fully polarized (un-polarized) current. For paramagnetic metal, $P=0$; and for half metal, $P=1$. The unpolarized current, I_u, carries no net spin polarization and obeys the conventional BTK theory. The remaining current, I_P, is entirely a quasiparticle current and can be calculated by allowing only non-Andreev processes at the point contact. More information can be found in the reference.[33]

IX. Discussions about the LCS on different contact conditions

The term “linear conductance structure” specifically refers to the spectroscopic feature, which is normally attributed to the inelastic tunneling effect in the barrier.[21,23] It usually exhibits a linear shape in a large bias voltage range, but may deviate from a straight line to a certain degree.[33-35] Also, the LCS may be asymmetric with respect to zero bias voltage.

The deviation from linearity at relatively high bias voltage has been reported previously.[33] A quadratic modification term ($|V|V$, where V is applied bias voltage) due to the contact condition was theoretically proposed to describe this deviation in the LCS, which is also asymmetric with respect to zero bias voltage.[35] And small differences in the spectra can be considered as a result of the different barrier conditions.[24,36,37] In our measurements, the small deviation from linearity appears over 80 meV (Fig. 2(c)) and is well above the gap size, which may consequently have a negligible effect on the gap structure. However, with this deviation from linearity in mind, we actually take the spectrum at the highest temperature in measurement as a background rather than a straight line to subtract the possible deviation from linearity. For example, in Fig. 2(c), the curve at 24 K (around T_N) is chosen as the background for subtraction to further analyze the gap structure at low temperatures.

The slight asymmetry is also present in PCS, which may partially be ascribed to the asymmetry of the LCS. The asymmetry of the spectra is a common feature in PCTS measurements, which has also been reported in previous works.[15,37-38] Theoretical explanations have been proposed by considering the position of the inelastic scattering center [33-35] in the barrier and the ratio of Fermi energy to the parameter of the tunneling barrier strength.[35] Therefore, the asymmetry of the PCS depends on the contact barrier, and the asymmetry of the spectra may vary from different point contact states.

X. Discussion about the Fermi level of $MnBi_2Te_4$ sample in our measurements

Previous studies have shown that the Fermi level in pristine $MnBi_2Te_4$ single crystals lies in the conduction band, and the exposure to the atmosphere would lead to significant hole doping in $MnBi_2Te_4$ samples.[29,39,40] In our measurements, the $MnBi_2Te_4$ single crystals are intentionally exposed to the atmosphere. Thus, the Fermi level should be pushed downward by the hole doping,

and approach the magnetic gap on the surface.

In our PCS, the minima of the dip structures are not exactly at zero bias voltage, which has also been reported before.[38] Additionally, the minima are distributed around zero bias, which is possibly due to that the Fermi level does not locate exactly in the middle of the gapped surface states. This Fermi level shift may be dependent on the specific contact condition, considering the inhomogeneous hole doping due to the oxidation and the possible electron transferring arising from the contact with metallic tips. It should be noted that no matter the minima of the dip structures are not exactly at zero bias voltage, abundant samples and point contact states are measured and the results of the surface gap are reproducible.

References

1. J H Li, Y Li, S Q. Du, Z Wang, B L Gu, S C Zhang, K He, W H Duan and Y Xu 2019 *Sci. Adv.* **5** eaaw5685
2. G E Blonder, M Tinkham and T M Klapwijk 1982 *Phys. Rev. B* **25** 4515
3. G Sheet, S Mukhopadhyay and P Raychaudhuri 2004 *Phys. Rev. B* **69** 134507
4. Y G Naidyuk and I K Yanson, Point-Contact Spectroscopy (Springer, New York, NY).
5. S Mukhopadhyay, P Raychaudhuri, D A Joshi and C V Tomy 2007 *Phys. Rev. B* **75** 014504
6. Yu G Naidyuk, 2018 *Low. Temp. Phys.* **44** 1806
7. T Le, L C Yin, Z L Feng, Q Huang, L Q Che, J Li, Y G Shi and X Lu 2019 *Phys. Rev. B* **99** 180504(R)
8. Y Huang, J Yan, Y L Wang, L Shan, Q Luo, W H Wang and H H Wen *2008 Supercond. Sci. Technol.* **21** 075011
9. W H Ko, M Kolmer, J Q Yan, A D Pham, M M Fu, F L üpke, S Okamoto, Z Gai, P Ganesh and A P Li 2020 *Phys. Rev. B* **102** 115402
10. H J Levinstein and J E Kunzler 1966 *Phys. Lett.* **20** 581
11. H J Levinstein, V G Chirba and J E Kunzler 1967 *Phys. Lett.* **24A** 362
12. C Berthod and T Giamarchi 2011 *Phys. Rev. B* **84** 15541
13. M E Hawley, K E Gray, B D Terris, H H Wang, K D Carlson and J M Williams *1986 Phys. Rev. Lett.* **57** 629

14. A A Sinchenko, Yu I Latyshev, S G Zybtsev, I G Gorlova and P Monceau 1999 *Phys. Rev. B* **60** 4624 (1999).

15. P Samuely, P Szabó, M Mihalika, N Hudáková and A A Menovsky 1996 *Physica B* **218** 185

16. J Aarts and A P Volodin 1995 *Physica B* **206&207** 43

17. A Fournel, J P Sorbier, M Konczykowski and P. Monceau 1986 *Phys. Rev. Lett* **57** 2199

18. K Luna, P Giraldo-Gallo, T Geballe, I Fisher and M Beasley 2014 *Phys. Rev. Lett.* **113** 177004

19. V Baltz, A D Naylor, K M Seemann, W Elder, S Sheen, K Westerholt, H Zabel, G Burnell, C H Marrows and B. J. Hickey 2009 *J. Phys.: Condens. Matter* **21** 09570

20. K H Bennemann, J B Ketterson, *Superconductivity: Volume 2: Novel Superconductors* (Springer, Berlin, 2008).

21. J R Kirtley and D J Scalapino 1990 *Phys. Rev. Lett.* **65** 79

22. V Baltz, A D Naylor, K M Seemann, W Elder, S Sheen, K Westerholt, H Zabel, G Burnell, C H Marrows and B. J. Hickey 2009 *J. Phys.: Condens. Matter* **21** 095701

23. P Seidel, M Grajcar and A Plecenik 1997 *Acta Phys. Pol.*, A **93** 355

24. X Chen, C Huan, Y S Hor, C A R S de Melo and Z Jiang 2012 arXiv: 1210.6054

25. Y J Deng, Y J Yu, M Z Shi, Z X Guo, Z H Xu, J Wang, X H Chen and Y B Zhang 2020 *Science* **367** 895

26. Y Gong, J W Guo, J H Li, K J Zhu, M H Liao, X Z Liu, Q H Zhang, L Gu, L Tang, X Feng, D Zhang, W Li, C L Song, L L Wang, P Yu, X Chen, Y Y Wang, H Yao, W H Duan, Y Xu, S C Zhang, X C Ma, Q K Xue and K. He 2019 *Chin. Phys. Lett.* **36** 076801

27. G He, Y L Jia, X Y Hou, Z X Wei, H D Xie, Z Z Yang, J N Shi, J Yuan, L Shan, B Y Zhu, H Li, L Gu, K Liu, T Xiang and K Jin 2017 *Phys. Rev. B* **95** 054510

28. D Q Zhang, M J Shi, T S Zhu, D Y Xing, H J Zhang and J Wang *2019 Phys. Rev. Lett.* **122** 206401

29. Y J Hao, P F Liu, Y Feng, X M Ma, E F Schwier, M Arita, S Kumar, C W Hu, R E Lu, M Zeng, Y Wang, Z Y Hao, H Y Sun, K Zhang, J W Mei, N Ni, L S Wu, K Shimada, C Y Chen, Q H Liu and C. Liu 2019 *Phys. Rev. X* **9** 041038

30. Y J Chen, L X Xu, J H Li, Y W Li, H Y Wang, C F Zhang, H Li, Y Wu, A J Liang, C Chen, S

W Jung, C Cacho, Y H Mao, S Liu, M X Wang, Y F Guo, Y Xu, Z K Liu, L X Yang and Y L Chen 2019 *Phys. Rev. X* **9** 041040

31. L Aggarwal, S Gayen, S Das, R Kumar, V Süß, C Felser, C Shekhar and G Sheet, *2017 Nat. Commun.* **8** 13974

32. O I Shklyarevskii, A M Duif, A G M Jansen and P Wyder 1986 *Phys. Rev. B* **34** 1956

33. R J Soulen Jr., J M Byers, M S Osofsky, B Nadgorny, T Ambrose, S F Cheng, P R Broussard, C T Tanaka, J Nowak, J S Moodera, A Barry and J. M. D. Coey 1998 *Science* **282** 85

34. J. R. Kirtley, S. Washburn, and D. J. Scalapino, Origin of the linear tunneling conductance background, 1992 *Phys. Rev. B* **45** 336

35. M Grajcar, A Plecenik, P Seidel, V Vojtanik and K U Barholz 1997 *Phys. Rev. B* **55** 11738

36. G I Rochlin and P K Hansma 1970 *Phys. Rev. B* **2** 1460

37. M Gurvitch, J M.Valles, Jr., A M Cucolo, R C Dynes, J P Garno, L F Schneemeyer and J V Waszczak 1989 Phys. Rev. Lett. **63** 1008

38. M E Hawley, K E Gray, D W Capone II and D G Hinks 1987 *Phys. Rev. B* **35** 7224

39. C Liu, Y C Wang, H Li, Y Wu, Y X Li, J H Li, K He, Y Xu, J S Zhang and Y Y Wang 2020 *Nat. Mater.* **19** 522

40. J Ge, Y Z. Liu, J H Li, H Li, T C. Luo, Y Wu, Y. Xu and J. Wang 2020 *Natl. Sci. Rev.* **7** 1280